PHILOSOPHICAL TRANSACTIONS A

rsta.royalsocietypublishing.org

Review

Cite this article: Wang C-C, Lai Y-H, Ou Y-M, Chang H-T, Wang Y-S. 2016 Critical factors determining the quantification capability of matrix-assisted laser desorption/ionization–time-of-flight mass spectrometry. *Phil. Trans. R. Soc. A* **374**: 20150371.
http://dx.doi.org/10.1098/rsta.2015.0371

Accepted: 17 May 2016

One contribution of 19 to a theme issue 'Quantitative mass spectrometry'.

Subject Areas:
analytical chemistry

Keywords:
ionization mechanism, timing characteristic, ion optics, detection efficiency, photoreaction, instrument parameters

Author for correspondence:
Yi-Sheng Wang
e-mail: wer@gate.sinica.edu.tw

Critical factors determining the quantification capability of matrix-assisted laser desorption/ionization–time-of-flight mass spectrometry

Chia-Chen Wang[1,2], Yin-Hung Lai[2], Yu-Meng Ou[2,3], Huan-Tsung Chang[3] and Yi-Sheng Wang[1,2]

[1]Department of Biochemistry, National Yang-Ming University, No. 155, Section 2, Linong Street, Taipei 112, Taiwan, Republic of China
[2]Genomics Research Center, Academia Sinica, 128 Academia Road, Section 2, Taipei 115, Taiwan, Republic of China
[3]Department of Chemistry, National Taiwan University, No. 1, Section 4, Roosevelt Road, Taipei 10617, Taiwan, Republic of China

Quantitative analysis with mass spectrometry (MS) is important but challenging. Matrix-assisted laser desorption/ionization (MALDI) coupled with time-of-flight (TOF) MS offers superior sensitivity, resolution and speed, but such techniques have numerous disadvantages that hinder quantitative analyses. This review summarizes essential obstacles to analyte quantification with MALDI-TOF MS, including the complex ionization mechanism of MALDI, sensitive characteristics of the applied electric fields and the mass-dependent detection efficiency of ion detectors. General quantitative ionization and desorption interpretations of ion production are described. Important instrument parameters and available methods of MALDI-TOF MS used for quantitative analysis are also reviewed.

This article is part of the themed issue 'Quantitative mass spectrometry'.

THE ROYAL SOCIETY PUBLISHING

1. Introduction

Quantifying molecular analytes is fundamental to scientific research and applications. Along with molecular identification, quantification reveals molecular information on physical and chemical properties as well as how molecules interact with their surroundings. Molecular abundance variations are also important indicators of chemical reactions, diseases and pollutants [1, see ch. 5, pp. 157–167 and chs. 10–13, pp. 249–331]. Among the important analytical techniques, mass spectrometry (MS) offers great accuracy, sensitivity and speed. In modern MS, a matrix-assisted laser desorption/ionization (MALDI) ion source coupled with a time-of-flight (TOF) mass spectrometer is one of the most widely used instruments for protein, carbohydrate and polymer studies. Quantification of analytes with MALDI-TOF MS, however, is highly challenging and should be done with care.

MALDI-TOF MS's ability to quantify the presence of different analytes depends on many factors. These factors are based on three MS components: the ion source, mass analyser and detector. Figure 1 depicts a typical configuration of a MALDI-TOF mass spectrometer. The MALDI ion source comprises a sample electrode and two extraction electrodes. The mass analyser contains an Einzel lens to focus the ion beam, deflector plates to adjust the ion trajectory, a mass gate (or timed ion selector) to suppress unwanted ions, and a reflectron to improve the mass resolving power. The most critical factor associated with the ion source is the ionization efficiency of the analytes. Such efficiency depends on the intrinsic properties of the analytes and ionization mechanisms. Sample morphologies also affect the reproducibility of spectra. In the mass analyser, quantitative capability is affected by ion transmission efficiency through the TOF mass analyser. Transmission efficiency reflects the configurations and timing characteristics of the electric fields used to guide the ions to the ion detectors. Ion lifetimes are also important, as ions spend most of their time in the TOF mass analyser [1, see ch. 5, pp. 157–167 and chs. 10–13, pp. 249–331]. The third factor is the detection efficiency of the ion detectors. On the whole, however, with properly and carefully designed experiments, including standard calibrations, quantitative analyses in MALDI-TOF MS can be achieved [2–4].

This review discusses the current status of analyte quantification with MALDI-TOF MS. The first part of this review discusses MALDI ionization and desorption mechanisms, including a general quantitative interpretation of ion yields based on chemical equilibria. The impact of mass spectrometric components and the methods used to obtain quantitative information are discussed in §3, including ways of improving the ion transmission efficiency through the TOF mass analyser and the detection properties of the ion detectors. Finally, in §4, current strategies for MALDI-TOF MS usage in quantitative measurement- and quantification-related issues are reviewed.

2. Ion production in matrix-assisted laser desorption/ionization

MALDI generates protonated (and deprotonated) analytes via complex reactions. To facilitate ionization, the analytes are typically dissolved in solution and co-crystallized with matrix compounds before measurements. After crystallization, ionization of analytes is achieved with photochemical reactions induced by a pulsed UV laser beam [5]. The initial photochemical reactions are followed by fast desorption of irradiated species from the solid to the gas phase. Decomposition of ions may occur if ions gain high internal energy through these processes.

The ionization efficiency of analytes depends on the matrix [6,7], analyte-to-matrix ratio [8,9], crystal morphology [10–13], laser energy [14,15] and others. Because no single experimental condition offers equal ionization efficiency for every analyte, a general reaction model is necessary for the optimization of experimental conditions in quantitative analysis. However, the MALDI reaction models proposed in the literature remain controversial owing to inconsistent experimental results. For example, the observed ion-to-neutral ratios of desorbed materials range from 10^{-3} to 10^{-8} [16–20]. This inconsistency is mainly attributed to the complexity of the ionization mechanisms.

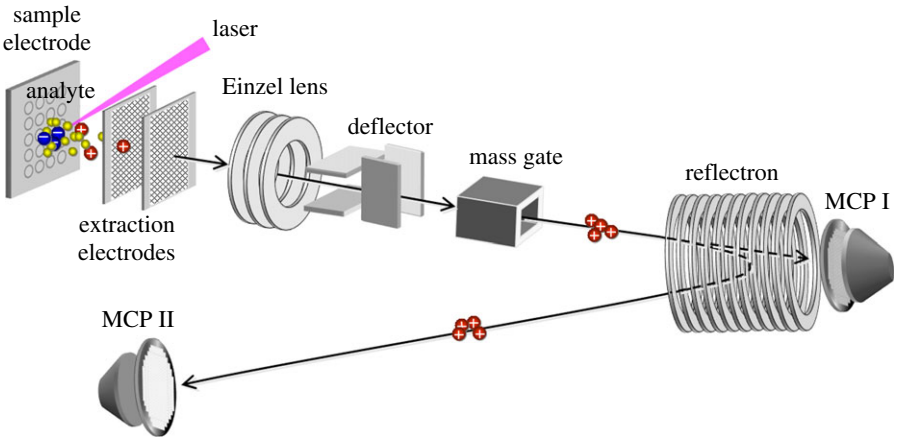

Figure 1. Configuration of MALDI-TOF mass spectrometer. The ion source comprises a sample electrode and two extraction electrodes. The mass analyser contains an Einzel lens, deflectors, a mass gate and a reflector. Ions are detected with MCP I and II in linear and reflectron modes, respectively. (Online version in colour.)

(a) Ionization

The ionization reactions in MALDI have been qualitatively described by numerous models. These models can be summarized into two categories: photoreaction and pre-charging. The pre-charging model proposes that analytes preserve their charges in solution after crystallization, and lasers serve as energy sources to liberate ions during the transition from the solid to the gas phase [21]. The pre-charging model is not included here because a quantitative interpretation of this model is not yet available. In the photoreaction model, on the other hand, the principal ionization reaction comprises two consecutive steps. The first step is the generation of matrix ions by photochemical reactions, and the second step is charge transfer from the matrix ions to neutral analytes [22–25]. For the initial ionization of matrices, two important reaction pathways are electron depletion [22,26,27], as shown in scheme 1, and proton disproportionation, as shown in scheme 2 [28–30].

$$\text{Scheme 1:} \quad \mathrm{M_{(s)}} + nh\nu \rightarrow \mathrm{M^*} \rightarrow \mathrm{M^{+\bullet}} + \mathrm{e^-}$$

$$\text{Scheme 2:} \quad 2\mathrm{M_{(s)}} + nh\nu \leftrightarrow 2\mathrm{M^*} \leftrightarrow [\mathrm{M}+\mathrm{H}]^+ + [\mathrm{M}-\mathrm{H}]^-$$

Here M and M* stand for matrices in the ground and excited electronic states, respectively. The matrix radical cation in scheme 1 undergoes complex ion–molecule reactions to produce protonated matrices. The early quantitative ionization model based on scheme 1 proposed that electron depletion is facilitated via multiphoton absorption or annihilation processes [31,32]. Knochenmuss proposed that three excited matrix molecules pool their energy to promote one of them to the ionization continuum [26,33]. By considering the decrease in the ionization energy of the matrix in the solid phase, Liu *et al.* demonstrated that electron depletion can be achieved by an energy corresponding to fewer than two UV photons [27].

In contrast with electron depletion, thermal or quasi-thermal ionization models were proposed to produce matrix proton pairs based on scheme 2 [28,30,34]. For example, Lai and co-workers estimated ion abundance based on chemical equilibrium between two 2,4,6-trihydroxyacetophenone (THAP) molecules,

$$2\mathrm{THAP} \overset{k_1}{\leftrightarrow} [\mathrm{THAP}+\mathrm{H}]^+ + [\mathrm{THAP}-\mathrm{H}]^-$$

The equilibrium constant (k_1) can be estimated from the predicted Gibbs free energy [28].

The second step of the photoreaction model is proton transfer from protonated matrices to neutral analytes via ion–molecule collision. Such reactive collisions occur numerously in the

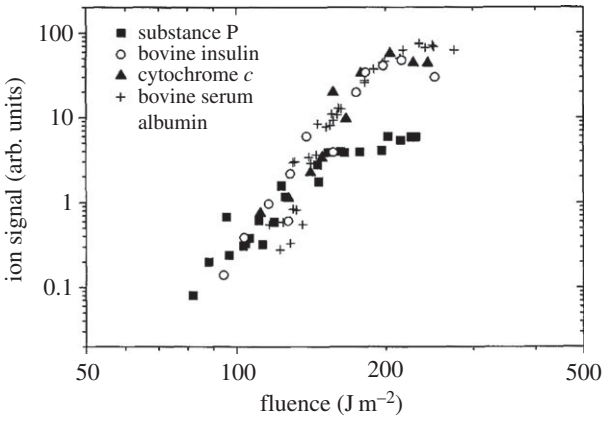

Figure 2. Change of ion abundance of various biomolecules with laser fluence. The result shows that ion signal intensity increases exponentially with the increase of laser fluence. (Reproduced with permission from Dreisewerd *et al.* [5] Copyright © 1995 Elsevier.)

initial phase-transition process. The efficiency of such proton-transfer reactions relies on the proton affinity (PA) of the analytes and matrices [22,35–37]. The higher the PA of the analyte, the higher the analyte ion yield is. For analytes with low PA, such as carbohydrates, ionization commonly forms alkali ion adducts [38,39]. Such ionization products are presumably produced via pre-charging reactions [21].

(b) Desorption

Desorption is mainly induced by sudden heating of matrix crystals during laser excitation. Desorption processes in MALDI have been described quantitatively in more detail than ionization [40–43]. The desorption efficiency of materials depends on the intrinsic properties of the samples and the excitation conditions, such as the molecular weight [43], crystal morphology [44–46] and laser conditions [5,47–49].

A comprehensive interpretation of ion yield should simultaneously consider ionization and desorption processes. Dreisewerd *et al.* [5] quantitatively described the desorption process by Arrhenius-type equations. In this interpretation, ion abundance (I_{ion}) is a function of desorption activation energy (E_{a}, J), initial crystal temperature (T_0, K) and laser fluence (F, J m^{-2}). By using transition state theory in the estimation of the desorption rate, Lai *et al.* [50] developed a comprehensive interpretation of ion yield:

$$I_{\mathrm{ion}} = A\frac{k(T_0+\gamma F)}{h}(1-\mathrm{e}^{-h\nu/k(T_0+\gamma F)})\,\mathrm{e}^{-E_{\mathrm{a}}/k(T_0+\gamma F)}[\mathrm{ion}]_{\mathrm{s}}, \tag{2.1}$$

Here, A is the pre-exponential factor, k is the Boltzmann constant, h is the Planck constant, γ is the conversion factor between laser fluence and surface temperature change, and ν is the vibrational frequency of the intermolecular bond. The concentration of surface ions $[\mathrm{ion}]_{\mathrm{s}}$ can be estimated using the equilibrium constant of the reactions in scheme 1 or 2. Observation shows crystal temperature rising instantaneously by approximately 1000 K and rapidly decreasing due to expansion cooling [51]. When the laser fluence is above the ion production threshold, the signal intensity increases exponentially with the increase in laser fluence, as shown in figure 2 [5]. As a high ion signal produced with high laser energy causes signal saturation, the best laser fluence for quantitative analysis is slightly above the threshold value [52].

(c) Decomposition

Ions produced in MALDI may decompose extensively because they typically have high internal energy. Decomposition results in unwanted ion loss and chemical noise that seriously affect the

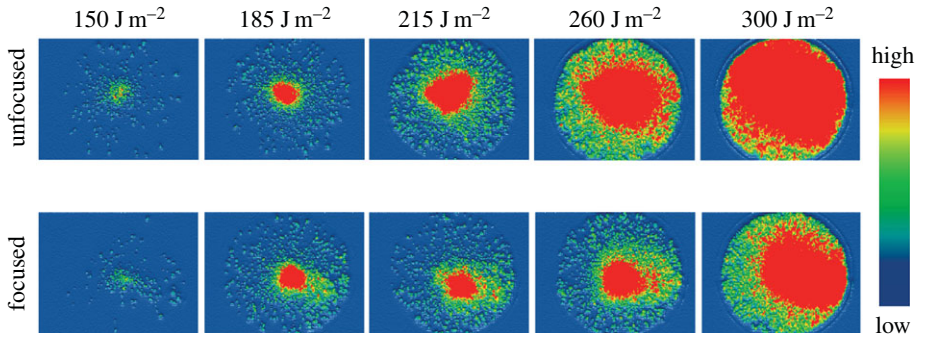

Figure 3. Spatial distribution of ions at detector surface under various experimental conditions. The upper row shows that ion distribution increases with laser fluence. The ion distribution exceeds that of the detection area with the highest laser fluence used in the measurement. The lower row shows that ion distribution can be reduced to obtain correct quantity information by using Einzel lens systems. (Reproduced with permission from Lai *et al.* [50]. Copyright © 2010 American Chemical Society.)

accuracy of quantitative analysis. Ion decomposition can be reduced by selecting 'soft' matrices [53] or decreasing the laser fluence [54].

3. Instrument performance

Instrument performance impacts quantification ability via the electric field and ion optics, ion extraction times and ion detection. Because individual ions exhibit distinct desorption properties and stability, their optimal extraction conditions in the ion source region vary. In TOF mass analysers, ion transmission is optimized with electrical components. The detection efficiency of ion detectors also critically affects the spectral pattern of MALDI-TOF MS data.

(a) Electric field and ion optics

Reliable quantitative information is available when proper ion transmission efficiency is achieved. Ion transmission efficiency reduces due to ion decomposition and poor ion trajectory. To suppress ion decomposition, as mentioned, the ionization conditions need to be changed. In addition, ions move both axially and radially after desorption [55], and the resultant expansion of the ion packets arriving at the detector increase with laser energy. Figure 3 gives ion populations for a 40 mm diameter detector surface using different laser fluences [50]. With an unfocused ion beam (upper row), a considerable portion of the ion beam misses the detection area when the highest laser fluence is used. Ion loss due to oversized distributions can be minimized using an Einzel lens and electrostatic deflectors to focus and adjust the ion beams (lower row), respectively [56,57]. To avoid signal saturation, as also mentioned above, it is important to use medium or low laser fluences.

(b) Timing characteristics of electric fields

MALDI-TOF MS sensitivity changes with the timing of ion extraction, or extraction delay. Delayed extraction is a well-established means of enhancing mass resolving power by reducing the spatial spread among ion packets during MALDI [58]. Another notable advantage is the significant suppression of metastable decay [59,60] due to the reduced number of ion–molecule collisions after extraction delay. Although higher sensitivity provides more accurate quantitative information, optimal extraction delay is mass-sensitive. Observations show that heavier ions require longer extraction delays and vice versa [61]. In this case, estimating analyte amounts based on relative signal intensity in MALDI-TOF MS is unreliable for ions with significant mass differences.

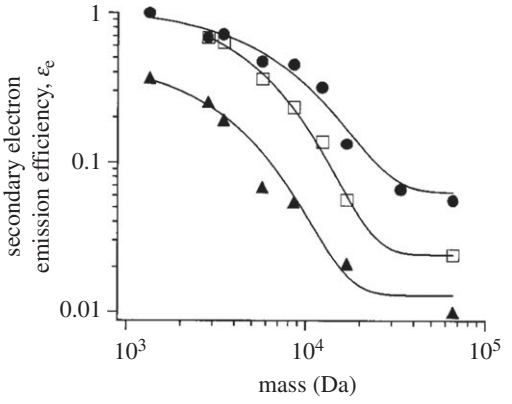

Figure 4. Change of secondary electron emission efficiency with ion mass and ion kinetic energy. The solid circles, open squares and solid triangles represent ion kinetic energy of 30, 20 and 10 keV, respectively. (Adapted from Westmacott *et al.* [68].)

The timing characteristics of mass gates (figure 1) also affect the accuracy of quantification. High-mass range sensitivity is dependent on ion detector saturation with lighter ions. In order to obtain a correct signal intensity for quantity estimations, all unwanted low-mass ions are deflected by appropriate timing of mass gating [62]. When examining proteins and peptides with MALDI-TOF MS, a low-mass cut-off is typically used to enhance the sensitivity for high-mass ions [63].

(c) Detector performance

MALDI-TOF mass analysers detect ions using microchannel plate (MCP) detectors [64]. An MCP detects incoming ions by amplifying secondary electrons ejected during high-velocity ion–surface collisions through a cascade reaction within microchannels. The resultant electric current collected by the anode is digitized. Thus, the detection efficiency of MCPs depends not only on the magnitude of amplification of secondary electrons, but more importantly on the conversion efficiency of primary ions to secondary electrons. A conventional single-disc MCP works when it is supplied with 600 V across the MCP. It reaches maximum gain (approx. 10^4) at 1000 V. As MCP signal intensity depends critically on the supplied voltage, it is important to ensure that the voltage supply does not vary.

Notably, operating MCPs in high-gain mode can easily cause saturation of microchannels when the secondary electron density reaches the space-charge limit [65], or when MCP surfaces are unable to deliver enough electric current to sustain an amplification reaction. Further, longer microchannels result in longer response times [64], which may distort the shape of the spectral signal, resulting in inaccurate peaks and signal intensity. If signal saturation or peak distortion occurs, ion abundance may be underestimated.

The conversion efficiency of secondary electrons from primary ions is mass-dependent [66–68]. Mass dependence varies with the efficiency of the MCP to generate secondary electrons, which in turn depends on ion velocity during MCP ion–surface collisions [68]. Figure 4 shows observed secondary electron yields with changing ion mass and ion kinetic energy [68]. As all ions possess the same kinetic energy, high-mass ions travel with lower speed than low-mass ions. This distinction in ion speed is the key principle behind TOF MS. Therefore, ions with higher mass generate fewer secondary electrons [69–71]. Although increasing acceleration voltage at the sample electrode restores high-mass ion detection efficiency, it is unable to compensate for the sensitivity difference between high- and low-mass ions. The only feasible way to account for this problem is by using internal standard compounds, which will be described in §4b.

When an ion enters a microchannel, amplification reactions proceed until all the secondary electrons exit the microchannel. Before amplification is complete, in a given microchannel, it is

unable to deliver amplification to another incoming ion. The period for a microchannel to fully recover is termed dead time, and it is typically in the millisecond range [64,72]. As most data acquisition times under MALDI-TOF MS are in the tens of microseconds, every microchannel can only receive one effective ion per acquisition event. Although MCP discs usually comprise a million microchannels, the dead time is still a property that needs to be considered in quantitative mass analysis [73]. If large numbers of ions are produced or the ion beam is focused on to a small area of the MCP, ion abundance may be considerably underestimated. Therefore, it is recommended to project ion beams across the entire area of the MCP.

Aside from the intrinsic properties of MCP detectors, accurate data analysis also depends on the properties of digitizers [74]. Electric signals delivered from MCPs are typically converted to electronic signals with analogue-to-digital (ADC) or time-to-digital (TDC) converters. An ADC directly converts electric currents to voltages, so ion abundance can be estimated based on the corresponding signal intensity. ADCs are suitable for detecting mid- to high-flux ion beams, but their accuracy in determining low-flux ion beams is limited by electronic noise. By contrast, TDCs count individual ions present at a time segment with typical resolution in the sub- to low-nanosecond range. TDCs are suitable for identifying low-flux ion beams, but ion abundance may be considerably underestimated if high ion flux is present. To achieve the highest analytical performance, it is possible to combine multiple digitizers in series [75,76]. Another novel strategy proposed is the use of an anode array (known as sectioned anodes) to collect electrons generated by MCPs [77,78].

4. Available methods

Quantitative analysis with MALDI-TOF MS is challenging because signal intensity in mass spectra varies with sample composition, sample morphology, laser conditions and depletion of samples during continuous laser exposure. Inhomogeneous sample morphology is also a crucial obstacle that leads to poor signal reproducibility (including the so-called sweet spot and coffee-ring effects) [79,80]. In order to perform quantitative analysis with the highest accuracy, it is important to find the optimal sample preparation method and to perform standard calibrations.

(a) Sample preparation methods

A major reason for poor reproducibility is inhomogeneous sample morphologies resulting from the dried-droplet (DD) method [43,81]. Such a problem is matrix-dependent. For example, samples prepared with THAP and α-cyano-4-hydroxycinnamic acid (CHCA) form homogeneous crystal morphologies, whereas those with 2,5-dihydroxybenzoic acid and sinapinic acid (SA) form irregular sample morphologies. To reduce data variation, hundreds of laser shots across randomly selected sample positions are used to obtain averaged spectra [82]. As CHCA provides higher ion yields than other matrices, it is the most commonly used matrix for quantitative studies [2,3,83]. Signal reproducibility is also improved by ionic liquid matrices [84,85], solvent-free sample preparation [86,87], small droplet deposition [88] and prestructured sample supports [89–91]. However, changing sample composition and preparation methods change ion yields, and the durability of prestructured sample supports is limited. Therefore, one has to compromise with all factors during analysis.

Alternatively, changing sample drying methods or surface properties change the resultant sample morphologies. Improved sample morphologies are available by preparing samples with fast evaporation [10,92], seeded layer (SL) [79,93], sandwich [94], electrospray deposition [95] and sublimation [44,96] methods. These methods provide fine and uniform crystals that provide superior signal reproducibility compared to conventional methods. Figure 5 shows the crystal morphologies of various matrices prepared with DD and SL methods [79]. With the SL method, significantly finer crystals than those with the DD method are produced. Drying samples under vacuum [97] or on a substrate with well-controlled surface and environmental temperatures [98] also provides finer sample homogeneity and signal reproducibility.

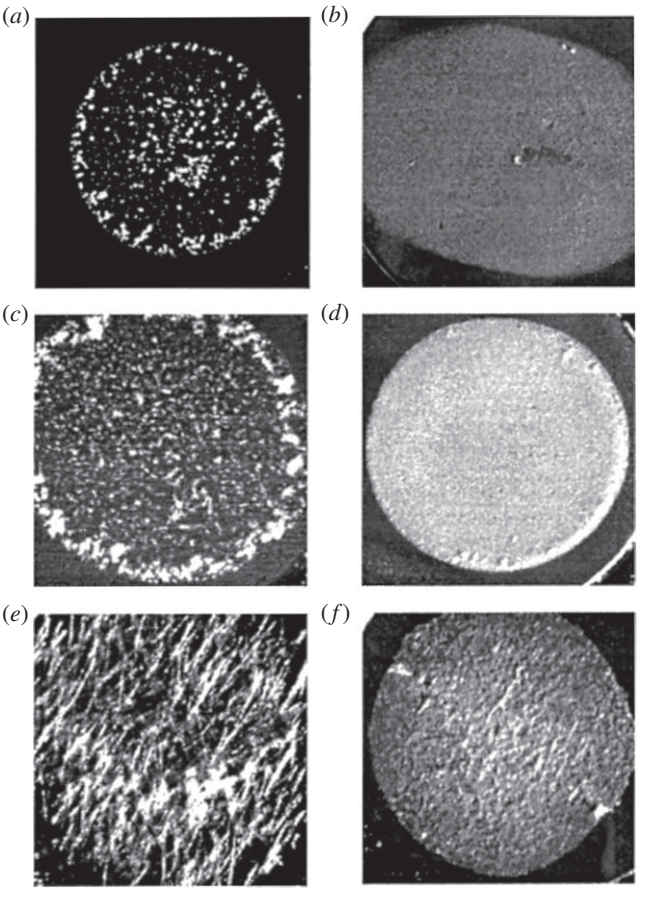

Figure 5. Crystal morphologies of three matrices prepared with DD and SL methods. (*a*) DD CHCA, (*b*) SL CHCA, (*c*) DD SA, (*d*) SL SA, (*e*) DD ferulic acid (FA) and (*f*) SL FA. (Adapted from Onnerfjord *et al.* [79].)

(b) Standard calibration

Standard calibration can be conducted externally or internally. In external calibration, the signal intensity of analytes is correlated to calibration curves determined with analytes of known concentration. However, external calibration may result in error because the ionization efficiencies of analytes change with composition. One such phenomenon is ion suppression effects observed in complex samples, especially when analysing trace analytes in biological fluids. On the other hand, internal calibration by mixing standard compounds in analyte mixtures minimizes uncertainties in quantitative analysis [99,100]. Ideal internal standards are compounds with similar chemical structures as the analyte. Isotopically labelled analyte analogues offer the best results for quantification analyses [4,101], including isotope-coded affinity tags [102], and isobaric tags for relative and absolute quantitation [103].

5. Conclusion

Quantitative analysis with MALDI-TOF MS is feasible but requires consideration of the sample and instrument conditions. The most critical problems are sample properties, ionization chemistry, electric fields and detector properties. Because the parameters are interrelated, adjusting one parameter changes the optimal conditions of others. Even though high-quality mass spectra can be obtained with optimal experimental conditions, quantitative analysis of MALDI-TOF mass spectra should be interpreted with special care. The most critical challenges

lie in ionization chemistry and detector efficiency. For example, the development of a universal matrix providing equal ionization efficiency to all analytes is highly necessary. On the other hand, new ion detectors providing equal efficiency to light and heavy ions and free of dead time problems are critical for improving data reliability.

Authors' contribution. C.-C.W., Y.-H.L. and Y.-M.O. summarized the literature articles, drafted and revised the manuscript; H.-T.C. supervised Y.-M.O. and reviewed the manuscript; and Y.-S.W. summarized the literature articles, drafted and prepared the final manuscript.

Competing interests. We declare we have no competing interests.

Funding. This work was supported by the Genomics Research Center, Academia Sinica and the Ministry of Science and Technology of Taiwan under contract no. 104-2119-M-001-014.

References

1. Urban P, Chen Y-C, Wang Y-S. 2016 *Time-resolved mass spectrometry*. New York, NY: Wiley.
2. Sleno L, Volmer DA. 2005 Some fundamental and technical aspects of the quantitative analysis of pharmaceutical drugs by matrix-assisted laser desorption/ionization mass spectrometry. *Rapid Commun. Mass Spectrom.* **19**, 1928–1936. (doi:10.1002/rcm.2006)
3. Szajli E, Feher T, Medzihradszky KF. 2008 Investigating the quantitative nature of MALDI-TOF MS. *Mol. Cell Proteomics* **7**, 2410–2418. (doi:10.1074/mcp.M800108-MCP200)
4. Bucknall M, Fung KYC, Duncan MW. 2002 Practical quantitative biomedical applications of MALDI-TOF mass spectrometry. *J. Am. Soc. Mass Spectrom.* **13**, 1015–1027. (doi:10.1016/s1044-0305(02)00426-9)
5. Dreisewerd K, Schurenberg M, Karas M, Hillenkamp F. 1995 Influence of the laser intensity and spot size on the desorption of molecules and ions in matrix-assisted laser desorption/ionization with a uniform beam profile. *Int. J. Mass Spectrom.* **141**, 127–148. (doi:10.1016/0168-1176(94)04108-j)
6. Krause J, Stoeckli M, Schlunegger UP. 1996 Studies on the selection of new matrices for ultraviolet matrix-assisted laser desorption/ionization time-of-flight mass spectrometry. *Rapid Commun. Mass Spectrom.* **10**, 1927–1933. (doi:10.1002/(SICI)1097-0231(199612)10:15<1927::AID-RCM709>3.0.CO;2-V)
7. Zenobi R, Knochenmuss R. 1998 Ion formation in MALDI mass spectrometry. *Mass Spectrom. Rev.* **17**, 337–366. (doi:10.1002/(SICI)1098-2787(1998)17:5<337::AID-MAS2>3.0.CO;2-S)
8. Yao J, Scott JR, Young MK, Wilkins CL. 1998 Importance of matrix : analyte ratio for buffer tolerance using 2,5-dihydroxybenzoic acid as a matrix in matrix-assisted laser desorption/ionization Fourier transform mass spectrometry and matrix-assisted laser desorption/ionization time of flight. *J. Am. Soc. Mass Spectrom.* **9**, 805–813. (doi:10.1016/s1044-0305(98)00046-4)
9. Tsai ST, Chen CH, Lee YT, Wang YS. 2008 Desorption dynamics of neutral molecules in matrix-assisted laser desorption/ionization. *Mol. Phys.* **106**, 239–247. (doi:10.1080/00268970701779671)
10. Vorm O, Roepstorff P, Mann M. 1994 Improved resolution and very high sensitivity in MALDI TOF of matrix surfaces made by fast evaporation. *Anal. Chem.* **66**, 3281–3287. (doi:10.1021/ac00091a044)
11. Chen Y, Vertes A. 2003 Pumping rate and surface morphology dependence of ionization processes in matrix-assisted laser desorption ionization. *J. Phys. Chem. A* **107**, 9754–9761. (doi:10.1021/jp035844u)
12. Shimma S, Takashima Y, Hashimoto J, Yonemori K, Tamura K, Hamada A. 2013 Alternative two-step matrix application method for imaging mass spectrometry to avoid tissue shrinkage and improve ionization efficiency. *J. Mass Spectrom.* **48**, 1285–1290. (doi:10.1002/jms.3288)
13. Westman A, Huthfehre T, Demirev P, Sundqvist BUR. 1995 Sample morphology effects in matrix-assisted laser desorption/ionization mass spectrometry of proteins. *J. Mass Spectrom.* **30**, 206–211. (doi:10.1002/jms.1190300131)
14. Westmacott G, Ens W, Hillenkamp F, Dreisewerd K, Schurenberg M. 2002 The influence of laser fluence on ion yield in matrix-assisted laser desorption ionization mass spectrometry. *Int. J. Mass Spectrom.* **221**, 67–81. (doi:10.1016/S1387-3806(02)00898-9)

15. Guenther S, Koestler M, Schulz O, Spengler B. 2010 Laser spot size and laser power dependence of ion formation in high resolution MALDI imaging. *Int. J. Mass Spectrom.* **294**, 7–15. (doi:10.1016/j.ijms.2010.03.014)
16. Tsai M-T, Lee S, Lu IC, Chu KY, Liang C-W, Lee CH, Lee YT, Ni C-K. 2013 Ion-to-neutral ratio of 2,5-dihydroxybenzoic acid in matrix-assisted laser desorption/ionization. *Rapid Commun. Mass Spectrom.* **27**, 955–963. (doi:10.1002/rcm.6534)
17. Bae YJ, Shin YS, Moon JH, Kim MS. 2012 Degree of ionization in MALDI of peptides: thermal explanation for the gas-phase ion formation. *J. Am. Soc. Mass Spectrom.* **23**, 1326–1335. (doi:10.1007/s13361-012-0406-y)
18. Ens W, Mao Y, Mayer F, Standing KG. 1991 Properties of matrix-assisted laser desorption measurements with a time-to-digital converter. *Rapid Commun. Mass Spectrom.* **5**, 117–123. (doi:10.1002/rcm.1290050306)
19. Mowry CD, Johnston MV. 1993 Simultaneous detection of ions and neutrals produced by matrix-assisted laser desorption. *Rapid Commun. Mass Spectrom.* **7**, 569–575. (doi:10.1002/rcm.1290070702)
20. Quist AP, Huthfehre T, Sundqvist BUR. 1994 Total yield measurements in matrix-assisted laser desorption using a quartz crystal microbalance. *Rapid Commun. Mass Spectrom.* **8**, 149–154. (doi:10.1002/rcm.1290080204)
21. Karas M, Kruger R. 2003 Ion formation in MALDI: the cluster ionization mechanism. *Chem. Rev.* **103**, 427–439. (doi:10.1021/cr010376a)
22. Ehring H, Karas M, Hillenkamp F. 1992 Role of photoionization and photochemistry in ionization processes of organic molecules and relevance for matrix-assisted laser desorption ionization mass spectrometry. *Org. Mass Spectrom.* **27**, 472–480. (doi:10.1002/oms.1210270419)
23. Liao PC, Allison J. 1995 Ionization processes in matrix-assisted laser desorption/ionization mass spectrometry: matrix-dependent formation of $[M+H]^+$ vs $[M+Na]^+$ ions of small peptides and some mechanistic comments. *J. Mass Spectrom.* **30**, 408–423. (doi:10.1002/jms.1190300304)
24. Breuker K, Knochenmuss R, Zhang J, Stortelder A, Zenobi R. 2003 Thermodynamic control of final ion distributions in MALDI: in-plume proton transfer reactions. *Int. J. Mass Spectrom.* **226**, 211–222. (doi:10.1016/S1387-3806(02)00965-X)
25. Knochenmuss R, Stortelder A, Breuker K, Zenobi R. 2000 Secondary ion–molecule reactions in matrix-assisted laser desorption/ionization. *J. Mass Spectrom.* **35**, 1237–1245. (doi:10.1002/1096-9888(200011)35:11<1237::AID-JMS74>3.0.CO;2-O)
26. Knochenmuss R. 2002 A quantitative model of ultraviolet matrix-assisted laser desorption/ionization. *J. Mass Spectrom.* **37**, 867–877. (doi:10.1002/jms.349)
27. Liu B-H, Charkin OP, Klemenko NM, Chen C-W, Wang Y-S. 2010 Initial ionization reaction in matrix-assisted laser desorption/ionization. *J. Phys. Chem. B* **114**, 10 853–10 859. (doi:10.1021/jp104178m)
28. Lai Y-H, Chen B-G, Lee YT, Wang Y-S, Lin SH. 2014 Contribution of thermal energy to initial ion production in matrix-assisted laser desorption/ionization observed with 2,4,6-trihydroxyacetophenone. *Rapid Commun. Mass Spectrom.* **28**, 1716–1722. (doi:10.1002/rcm.6952)
29. Chu KY, Lee S, Tsai MT, Lu IC, Dyakov YA, Lai YH, Lee YT, Ni CK. 2014 Thermal proton transfer reactions in ultraviolet matrix-assisted laser desorption/ionization. *J. Am. Soc. Mass Spectrom.* **25**, 310–318. (doi:10.1007/s13361-013-0792-9)
30. Bae YJ, Kim MS. 2015 A thermal mechanism of ion formation in MALDI. *Annu. Rev. Anal. Chem.* **8**, 41–60. (doi:10.1146/annurev-anchem-081413-024102)
31. Ludemann HC, Redmond RW, Hillenkamp F. 2002 Singlet–singlet annihilation in ultraviolet matrix-assisted laser desorption/ionization studied by fluorescence spectroscopy. *Rapid Commun. Mass Spectrom.* **16**, 1287–1294. (doi:10.1002/rcm.712)
32. Allwood DA, Dyer PE, Dreyfus RW. 1997 Ionization modelling of matrix molecules in ultraviolet matrix-assisted laser desorption/ionization. *Rapid Commun. Mass Spectrom.* **11**, 499–503. (doi:10.1002/(SICI)1097-0231(199703)11:5<499::AID-RCM880>3.0.CO;2-2)
33. Knochenmuss R. 2003 A quantitative model of ultraviolet matrix-assisted laser desorption/ionization including analyte ion generation. *Anal. Chem.* **75**, 2199–2207. (doi:10.1021/ac034032r)

34. Lu IC, Lee C, Lee YT, Ni CK. 2015 Ionization mechanism of matrix-assisted laser desorption/ionization. *Annu. Rev. Anal. Chem.* **8**, 21–39. (doi:10.1146/annurev-anchem-071114-040315)
35. Harrison AG. 1997 The gas-phase basicities and proton affinities of amino acids and peptides. *Mass Spectrom. Rev.* **16**, 201–217. (doi:10.1002/(SICI)1098-2787(1997)16:4<201::AID-MAS3>3.0.CO;2-L)
36. Jebber KA, Zhang K, Cassady CJ, Chung-Phillips A. 1996 Ab initio and experimental studies on the protonation of glucose in the gas phase. *J. Am. Chem. Soc.* **118**, 10 515–10 524. (doi:10.1021/Ja960427z)
37. Knochenmuss R. 2006 Ion formation mechanisms in UV-MALDI. *Analyst* **131**, 966–986. (doi:10.1039/b605646f)
38. Mohr MD, Bornsen KO, Widmer HM. 1995 Matrix-assisted laser-desorption ionization mass-spectrometry—improved matrix for oligosaccharides. *Rapid Commun. Mass Spectrom.* **9**, 809–814. (doi:10.1002/rcm.1290090919)
39. Zhang J, Ha TK, Knochenmuss R, Zenobi R. 2002 Theoretical calculation of gas-phase sodium binding energies of common MALDI matrices. *J. Phys. Chem. A* **106**, 6610–6617. (doi:10.1021/Jp0203548)
40. Vertes A, Irinyi G, Gijbels R. 1993 Hydrodynamic model of matrix-assisted laser-desorption mass-spectrometry. *Anal. Chem.* **65**, 2389–2393. (doi:10.1021/Ac00065a036)
41. Johnson RE. 1994 Models for matrix-assisted desorption by a laser-pulse. *Int. J. Mass Spectrom.* **139**, 25–38. (doi:10.1016/0168-1176(94)04070-2)
42. Zhigilei LV, Leveugle E, Garrison BJ, Yingling YG, Zeifman MI. 2003 Computer simulations of laser ablation of molecular substrates. *Chem. Rev.* **103**, 321–347. (doi:10.1021/cr010459r)
43. Dreisewerd K. 2003 The desorption process in MALDI. *Chem. Rev.* **103**, 395–425. (doi:10.1021/cr010375i)
44. Jaskolla TW, Karas M, Roth U, Steinert K, Menzel C, Reihs K. 2009 Comparison between vacuum sublimed matrices and conventional dried droplet preparation in MALDI-TOF mass spectrometry. *J. Am. Soc. Mass Spectrom.* **20**, 1104–1114. (doi:10.1016/j.jasms.2009.02.010)
45. Gluckmann M, Pfenninger A, Kruger R, Thierolf M, Karas M, Horneffer V, Hillenkamp F, Strupat K. 2001 Mechanisms in MALDI analysis: surface interaction or incorporation of analytes? *Int. J. Mass Spectrom.* **210**, 121–132. (doi:10.1016/s1387-3806(01)00450-x)
46. Horneffer V, Dreisewerd K, Ludemann HC, Hillenkamp F, Lage M, Strupat K. 1999 Is the incorporation of analytes into matrix crystals a prerequisite for matrix-assisted laser desorption/ionization mass spectrometry? A study of five positional isomers of dihydroxybenzoic acid. *Int. J. Mass Spectrom.* **185**, 859–870. (doi:10.1016/s1387-3806(98)14218-5)
47. Little MW, Laboy J, Murray KK. 2007 Wavelength dependence of soft infrared laser desorption and ionization. *J. Phys. Chem. C* **111**, 1412–1416. (doi:10.1021/jp063154v)
48. Soltwisch J, Jaskolla TW, Dreisewerd K. 2013 Color matters—material ejection and ion yields in UV-MALDI mass spectrometry as a function of laser wavelength and laser fluence. *J. Am. Soc. Mass Spectrom.* **24**, 1477–1488. (doi:10.1007/s13361-013-0699-5)
49. Nordhoff E, Ingendoh A, Cramer R, Overberg A, Stahl B, Karas M, Hillenkamp F, Crain PF. 1992 Matrix-assisted laser desorption ionization mass-spectrometry of nucleic-acids with wavelengths in the ultraviolet and infrared. *Rapid Commun. Mass Spectrom.* **6**, 771–776. (doi:10.1002/rcm.1290061212)
50. Lai Y-H, Wang C-C, Lin S-H, Lee Y-T, Wang Y-S. 2010 Solid-phase thermodynamic interpretation of ion desorption in matrix-assisted laser desorption/ionization. *J. Phys. Chem. B* **114**, 13 847–13 852. (doi:10.1021/jp104250g)
51. Koubenakis A, Frankevich V, Zhang J, Zenobi R. 2004 Time-resolved surface temperature measurement of MALDI matrices under pulsed UV laser irradiation. *J. Phys. Chem. A* **108**, 2405–2410. (doi:10.1021/Jp037811k)
52. Williams TL, Andrzejewski D, Lay JO, Musser SM. 2003 Experimental factors affecting the quality and reproducibility of MALDI TOF mass spectra obtained from whole bacteria cells. *J. Am. Soc. Mass Spectrom.* **14**, 342–351. (doi:10.1016/S1044-0305(03)00065-5)
53. Schulz E, Karas M, Rosu F, Gabelica V. 2006 Influence of the matrix on analyte fragmentation in atmospheric pressure MALDI. *J. Am. Soc. Mass Spectrom.* **17**, 1005–1013. (doi:10.1016/j.jasms.2006.03.009)

54. Luo GH, Marginean I, Vertes A. 2002 Internal energy of ions generated by matrix-assisted laser desorption/ionization. *Anal. Chem.* **74**, 6185–6190. (doi:10.1021/Ac020339z)
55. Zhang W, Chait BT. 1997 Radial velocity distributions of molecular ions produced by matrix-assisted laser desorption/ionization. *Int. J. Mass Spectrom. Ion Process.* **160**, 259–267. (doi:10.1016/S0168-1176(96)04526-0)
56. Mamyrin BA, Karataev VI, Shmikk DV, Zagulin VA. 1973 Mass-reflectron a new nonmagnetic time-of-flight high-resolution mass-spectrometer. *Zh. Eksp. Teor. Fiz.* **64**, 82–89.
57. Jonsson G, Hedin A, Håkansson P, Sundqvist BUR, Bennich H, Roepstorff P. 1989 Compensation for non-normal ejection of large molecular ions in plasma-desorption mass spectrometry. *Rapid Commun. Mass Spectrom.* **3**, 190–191. (doi:10.1002/rcm.1290030607)
58. Cotter RJ. 1997 Pulsed extraction, continuous ionization, and ion storage instruments. In *Time of flight mass spectrometry: instrumentation and applications in biological research*, pp. 137–168. Washington, DC: American Chemical Society.
59. Kaufmann R, Chaurand P, Kirsch D, Spengler B. 1996 Post-source decay and delayed extraction in matrix-assisted laser desorption/ionization-reflectron time-of-flight mass spectrometry. Are there trade-offs? *Rapid Commun. Mass Spectrom.* **10**, 1199–1208. (doi:10.1002/(SICI)1097-0231(19960731)10:10<1199::AID-RCM643>3.0.CO;2-F)
60. Tsarbopoulos A, Bahr U, Pramanik BN, Karas M. 1997 Glycoprotein analysis by delayed extraction and post-source decay MALDI-TOF-MS. *Int. J. Mass Spectrom.* **169**, 251–261. (doi:10.1016/S0168-1176(97)00222-X)
61. Barbacci DC, Edmondson RD, Russell DH. 1997 Evaluation of the variables that affect resolution in delayed extraction MALDI-TOF. *Int. J. Mass Spectrom.* **165**, 221–235. (doi:10.1016/S0168-1176(97)00169-9)
62. Hanson CD, Just CL. 1994 Selective background suppression in MALDI-TOF mass-spectrometry. *Anal. Chem.* **66**, 3676–3680. (doi:10.1021/Ac00093a022)
63. Beavis RC, Chait BT. 1989 Factors affecting the ultraviolet laser desorption of proteins. *Rapid Commun. Mass Spectrom.* **3**, 233–237. (doi:10.1002/rcm.1290030708)
64. Wiza JL. 1979 Microchannel plate detectors. *Nucl. Instrum. Methods* **162**, 587–601. (doi:10.1016/0029-554X(79)90734-1)
65. Westman A, Brinkmalm G, Barofsky DF. 1997 MALDI induced saturation effects in chevron microchannel plate detectors. *Int. J. Mass Spectrom. Ion Process.* **169–170**, 79–87. (doi:10.1016/S0168-1176(97)00205-X)
66. Geno PW, Macfarlane RD. 1989 Secondary-electron emission induced by impact of low-velocity molecular-ions on a microchannel plate. *Int. J. Mass Spectrom. Ion Process.* **92**, 195–210. (doi:10.1016/0168-1176(89)83028-9)
67. Meier R, Eberhardt P. 1993 Velocity and ion species dependence of the gain of microchannel plates. *Int. J. Mass Spectrom. Ion Process.* **123**, 19–27. (doi:10.1016/0168-1176(93)87050-3)
68. Westmacott G, Frank M, Labov SE, Benner WH. 2000 Using a superconducting tunnel junction detector to measure the secondary electron emission efficiency for a microchannel plate detector bombarded by large molecular ions. *Rapid Commun. Mass Spectrom.* **14**, 1854–1861. (doi:10.1002/1097-0231(20001015)14:19<1854::AID-RCM102>3.0.CO;2-M)
69. Martens J, Ens W, Standing KG, Verentchikov A. 1992 Secondary-ion and electron production from surfaces bombarded by large polyatomic ions. *Rapid Commun. Mass Spectrom.* **6**, 147–157. (doi:10.1002/rcm.1290060215)
70. Brunelle A, Chaurand P, Della-Negra S, Le Beyec Y, Baptista GB. 1993 Surface secondary electron and secondary ion emission induced by large molecular ion impacts. *Int. J. Mass Spectrom. Ion Process.* **126**, 65–73. (doi:10.1016/0168-1176(93)80071-L)
71. Verentchikov A, Ens W, Martens J, Standing KG. 1993 Detection of large molecular ions by secondary ion and secondary electrom emission. *Int. J. Mass Spectrom. Ion Process.* **126**, 75–83. (doi:10.1016/0168-1176(93)80072-M)
72. Seko A, Kobayashi H. 1973 Application of channel multiplier plates as image information preprocessors. *Rev. Sci. Instrum.* **44**, 400–405. (doi:10.1063/1.1686143)
73. Wei S, Tzeng WB, Castleman AW. 1990 Dissociation dynamics: measurements of decay fractions of metastable ammonia cluster ions. *J. Chem. Phys.* **93**, 2506–2512. (doi:10.1063/1.459033)
74. Da Costa G, Vurpillot F, Bostel A, Bouet M, Deconihout B. 2005 Design of a delay-line position-sensitive detector with improved performance. *Rev. Sci. Instrum.* **76**, 013304. (doi:10.1063/1.1829975)

75. Baptista GB, Brunelle A, Chaurand P, Della-Negra S, Depauw J, Le Bayec Y, Chait BT. 1991 Ion counting and ion intensity measurements in time-of-flight mass spectrometry. Application to matrix-assisted laser desorption. *Rapid Commun. Mass Spectrom.* **5**, 632–637. (doi:10.1002/rcm.1290051214)
76. Beavis RC. 1996 Increasing the dynamic range of a transient recorder by using two analog-to-digital converters. *J. Am. Soc. Mass Spectrom.* **7**, 107–113. (doi:10.1016/1044-0305(95)00592-7)
77. Bouneau S, Cohen P, Della Negra S, Jacquet D, Le Beyec Y, Le Bris J, Pautrat M, Sellem R. 2003 256-Anode channel plate device for simultaneous ion detection in time of flight measurements. *Rev. Sci. Instrum.* **74**, 57–67. (doi:10.1063/1.1527721)
78. Barbacci DC, Russell DH, Schultz JA, Holocek J, Ulrich S, Burton W, Van Stipdonk M. 1998 Multi-anode detection in electrospray ionization time-of-flight mass spectrometry. *J. Am. Soc. Mass Spectrom.* **9**, 1328–1333. (doi:10.1016/S1044-0305(98)00113-5)
79. Onnerfjord P, Ekstrom S, Bergquist J, Nilsson J, Laurell T, Marko-Varga G. 1999 Homogeneous sample preparation for automated high throughput analysis with matrix-assisted laser desorption/ionisation time-of-flight mass spectrometry. *Rapid Commun. Mass Spectrom.* **13**, 315–322. (doi:10.1002/(SICI)1097-0231(19990315)13:5<315::AID-RCM483>3.0.CO;2-C)
80. Albrethsen J. 2007 Reproducibility in protein profiling by MALDI-TOF mass spectrometry. *Clin. Chem.* **53**, 852–858. (doi:10.1373/clinchem.2006.082644)
81. Garden RW, Sweedler JV. 2000 Heterogeneity within MALDI samples as revealed by mass spectrometric imaging. *Anal. Chem.* **72**, 30–36. (doi:10.1021/ac9908997)
82. Chaurand P, Schwartz SA, Reyzer ML, Caprioli RA. 2005 Imaging mass spectrometry: principles and potentials. *Toxicol. Pathol.* **33**, 92–101. (doi:10.1080/01926230590881862)
83. Sleno L, Volmer DA. 2006 Assessing the properties of internal standards for quantitative matrix-assisted laser desorption/ionization mass spectrometry of small molecules. *Rapid Commun. Mass Spectrom.* **20**, 1517–1524. (doi:10.1002/rcm.2498)
84. Zabet-Moghaddam M, Heinzle E, Tholey A. 2004 Qualitative and quantitative analysis of low molecular weight compounds by ultraviolet matrix-assisted laser desorption/ionization mass spectrometry using ionic liquid matrices. *Rapid Commun. Mass Spectrom.* **18**, 141–148. (doi:10.1002/Rcm.1293)
85. Li YL, Gross ML. 2004 Ionic-liquid matrices for quantitative analysis by MALDI-TOF mass spectrometry. *J. Am. Soc. Mass Spectrom.* **15**, 1833–1837. (doi:10.1016/j.jasms.2004.08.011)
86. Trimpin S, Keune S, Rader HJ, Mullen K. 2006 Solvent-free MALDI-MS: developmental improvements in the reliability and the potential of MALDI in the analysis of synthetic polymers and giant organic molecules. *J. Am. Soc. Mass Spectrom.* **17**, 661–671. (doi:10.1016/j.jasms.2006.01.007)
87. Trimpin S, Weidner SM, Falkenhagen J, McEwen CN. 2007 Fractionation and solvent-free MALDI-MS analysis of polymers using liquid adsorption chromatography at critical conditions in combination with a multisample on-target homogenization/transfer sample preparation method. *Anal. Chem.* **79**, 7565–7570. (doi:10.1021/ac070986w)
88. Tu T, Sauter ADJ, Sauter ADR, Gross ML. 2008 Improving the signal intensity and sensitivity of MALDI mass spectrometry by using nanoliter spots deposited by induction-based fluidics. *J. Am. Soc. Mass Spectrom.* **19**, 1086–1090. (doi:10.1016/j.jasms.2008.03.017)
89. Schuerenbeg M, Luebbert C, Eickhoff H, Kalkum M, Lehrach H, Nordhoff E. 2000 Prestructured MALDI-MS sample supports. *Anal. Chem.* **72**, 3436–3442. (doi:10.1021/Ac000092a)
90. Urban PL, Jefimovs K, Amantonico A, Fagerer SR, Schmid T, Madler S, Puigmarti-Luis J, Goedecke N, Zenobi R. 2010 High-density micro-arrays for mass spectrometry. *Lab on a Chip* **10**, 3206–3209. (doi:10.1039/c0lc00211a)
91. Hu J-B, Chen Y-C, Urban PL. 2013 Coffee-ring effects in laser desorption/ionization mass spectrometry. *Anal. Chim. Acta* **766**, 77–82. (doi:10.1016/j.aca.2012.12.044)
92. Nicola AJ, Gusev AI, Proctor A, Jackson EK, Hercules DM. 1995 Application of the fast-evaporation sample preparation method for improving quantification of angiotensin-II by matrix-assisted laser-desorption ionization. *Rapid Commun. Mass Spectrom.* **9**, 1164–1171. (doi:10.1002/rcm.1290091216)
93. Dai YQ, Whittal RM, Li L. 1999 Two-layer sample preparation: a method for MALDI-MS analysis of complex peptide and protein mixtures. *Anal. Chem.* **71**, 1087–1091. (doi:10.1021/ac980684h)

94. Li L, Golding RE, Whittal RM. 1996 Analysis of single mammalian cell lysates by mass spectrometry. *J. Am. Chem. Soc.* **118**, 11 662–11 663. (doi:10.1021/ja9627499)
95. Hensel RR, King RC, Owens KG. 1997 Electrospray sample preparation for improved quantitation in matrix-assisted laser desorption/ionization time-of-flight mass spectrometry. *Rapid Commun. Mass Spectrom.* **11**, 1785–1793. (doi:10.1002/(SICI)1097-0231(19971030)11:16<1785::AID-RCM78>3.0.CO;2-Q)
96. Hankin JA, Barkley RM, Murphy RC. 2007 Sublimation as a method of matrix application for mass spectrometric imaging. *J. Am. Soc. Mass Spectrom.* **18**, 1646–1652. (doi:10.1016/j.jasms.2007.06.010)
97. Cohen SL, Chait BT. 1996 Influence of matrix solution conditions on the MALDI-MS analysis of peptides and proteins. *Anal. Chem.* **68**, 31–37. (doi:10.1021/Ac9507956)
98. Lai Y-H, Cai Y-H, Lee H, Ou Y-M, Hsiao C-H, Tsao C-W, Chang H-T, Wang Y-S. 2016 Reducing spatial heterogeneity of MALDI samples with Marangoni flows during sample preparation. *J. Am. Soc. Mass Spectrom.* **27**, 1314–1321. (doi:10.1007/s13361-016-1406-0)
99. Kang MJ, Tholey A, Heinzle E. 2001 Application of automated matrix-assisted laser desorption/ionization time-of-flight mass spectrometry for the measurement of enzyme activities. *Rapid Commun. Mass Spectrom.* **15**, 1327–1333. (doi:10.1002/rcm.376)
100. Gusev AI, Wilkinson WR, Proctor A, Hercules DM. 1996 Direct quantitative analysis of peptides using matrix assisted laser desorption ionization. *Fresenius J. Anal. Chem.* **354**, 455–463. (doi:10.1007/s0021663540455)
101. Mirgorodskaya OA, Kozmin YP, Titov MI, Korner R, Sonksen CP, Roepstorff P. 2000 Quantitation of peptides and proteins by matrix-assisted laser desorption/ionization mass spectrometry using ^{18}O-labeled internal standards. *Rapid Commun. Mass Spectrom.* **14**, 1226–1232. (doi:10.1002/1097-0231(20000730)14:14<1226::AID-RCM14>3.3.CO;2-M)
102. Griffin TJ, Gygi SP, Rist B, Aebersold R, Loboda A, Jilkine A, Ens W, Standing KG. 2001 Quantitative proteomic analysis using a MALDI quadrupole time-of-flight mass spectrometer. *Anal. Chem.* **73**, 978–986. (doi:10.1021/ac001169y)
103. Wiese S, Reidegeld KA, Meyer HE, Warscheid B. 2007 Protein labeling by iTRAQ: a new tool for quantitative mass spectrometry in proteome research. *Proteomics* **7**, 340–350. (doi:10.1002/pmic.200600422)